NASA TECHNICAL MEMORANDUM

NASA TM X-72,751

NASA TM X-72,751

(NASA-TM-X-72751) A NUMERICAL METHOD FOR DETERMINING THE NATURAL VIBRATION CHARACTERISTICS OF ROTATING NONUNIFORM CANTILEVER BLADES (NASA) 36 p HC $3.75 CSCL 13M G3/39

N76-10505

Unclas

39462

A NUMERICAL METHOD FOR DETERMINING THE NATURAL VIBRATION CHARACTERISTICS OF ROTATING NONUNIFORM CANTILEVER BLADES

William F. White, Jr.
Langley Directorate
U.S. Army Air Mobility R&D Laboratory
NASA-Langley Research Center
Hampton, Virginia 23665

and

Raymond E. Malatino
Naval Air Systems Command
Washington, D. C. 20361

NATIONAL AERONAUTICS AND SPACE ADMINISTRATION
LANGLEY RESEARCH CENTER, HAMPTON, VIRGINIA 23665

1. Report No.	2. Government Accession No.	3. Recipient's Catalog No.
NASA TMX 72,751		

4. Title and Subtitle	5. Report Date
A Numerical Method for Determining the Natural Vibration Characteristics of Rotating Nonuniform Cantilever Blades	OCTOBER 1975
	6. Performing Organization Code
7. Author(s) William F. White, Jr.-US Army Air Mobility R&D Lab Raymond E. Malatino-Naval Air Systems Command	8. Performing Organization Report No.
	10. Work Unit No.
9. Performing Organization Name and Address NASA-Langley Research Center Hampton, VA 23665	11. Contract or Grant No.
	13. Type of Report and Period Covered Technical Memorandum
12. Sponsoring Agency Name and Address National Aeronautics and Space Administration Washington, DC 20546	14. Sponsoring Agency Code

15. Supplementary Notes

16. Abstract

A method is presented for determining the free vibration characteristics of a rotating blade having nonuniform spanwise properties and cantilever boundary conditions. The equations which govern the coupled flapwise, chordwise, and torsional motion of such a blade are solved using an integrating matrix method. By expressing the equations of motion in matrix notation, utilizing the integrating matrix as an operator, and applying the boundary conditions, the equations are formulated into an eigenvalue problem whose solutions may be determined by conventional methods. Computed results are compared with experimental data.

17. Key Words (Suggested by Author(s)) (STAR category underlined)	18. Distribution Statement
Natural vibrations Rotating beams Integrating matrix Eigenvalue problem	Unclassified - Unlimited

19. Security Classif. (of this report)	20. Security Classif. (of this page)	21. No. of Pages	22. Price*
Unclassified	Unclassified	34	$3.75

*Available from { The National Technical Information Service, Springfield, Virginia 22151
STIF/NASA Scientific and Technical Information Facility, P.O. Box 33, College Park, MD 20740

A NUMERICAL METHOD FOR DETERMINING THE NATURAL

VIBRATION CHARACTERISTICS OF ROTATING NONUNIFORM CANTILEVER BLADES

William F. White, Jr.
Langley Directorate
U.S. Army Air Mobility R&D Laboratory
NASA Langley Research Center
Hampton, Virginia 23665

and

Raymond E. Malatino
Naval Air Systems Command
Washington, D.C. 20361

SUMMARY

A method is presented for determining the free vibration characteristics of a rotating blade having nonuniform spanwise properties and cantilever boundary conditions. The equations which govern the coupled flapwise, chordwise, and torsional motion of such a blade are solved using an integrating matrix method. By expressing the equations of motion in matrix notation, utilizing the integrating matrix as an operator, and applying the boundary conditions, the equations are formulated into an eigenvalue problem whose solutions may be determined by conventional methods. Computed results are compared with experimental data.

INTRODUCTION

Natural vibration characteristics of rotating blades are of fundamental importance from the viewpoint of flying qualities, blade life, vibration levels, and stability. Helicopters, propellers, and turbines may have serious resonant vibration problems when the excitation frequencies are equal to some multiple of the rotational speed. To insure that conditions susceptible to resonance do not exist within the range of operating speeds, it is necessary that the natural frequencies be determined accurately. Also, the natural modes, because of their orthogonality relationships, are often used in forced response and stability calculations.

This paper formulates a numerical solution of the natural vibration frequencies and mode shapes of rotating nonuniform blades. This problem has been treated analytically in a very complete development by Houbolt and Brooks.[1] However, very few results are presented, and they are for special cases of limited interest. Numerous other studies[2-14] have investigated various facets of the problem using a variety of numerical solution methods. Generally, these studies may be classified as investigations of a subset of the governing equations derived in Reference 1. The present analysis employs the governing equations derived in Reference 1. The integrating matrix as developed by Hunter[10] is the basis for the present method of solution. The integrating matrix is a means of numerically integrating a function that is expressed in terms of the values of the function at increments of the independent variable. It is derived by expressing the integrand as a polynomial in the form of Newton's forward-difference interpolation formula.

The equations of motion which are linear homogeneous equations having variable coefficients are expressed in matrix form using the integrating matrix. The boundary conditions are applied and the resulting matrix equations expressed in standard eigenvalue form. Solutions to this eigenvalue problem may be obtained by conventional methods. In developing the solution, all functions are in effect represented by seventh-degree polynomials at the boundaries as well as elsewhere on the beam. Since the polynomials approximate the functions very accurately, the integration of these polynomial representations yield extremely small errors.[10] The method is appealing because the numerical solution may be formulated quickly from the governing equations and may be easily programmed for computations by a digital computer.

SYMBOLS

B_1, B_2	Blade section constants
E	Young's modulus of elasticity
EI_t/EI_o	Ratio of tip to root bending modulus
e	Distance between mass and elastic axis, positive when mass axis lies ahead of elastic axis
e_a	Distance between area centroid of tensile member and elastic axis, positive for centroid forward
G	Shear modulus of elasticity
I_1, I_2	Cross-section area moments of inertia
J	Torsional stiffness constant
k_a	Polar radius of gyration of cross-sectional area effective in carrying tension
k_m	Polar radius of gyration of cross-sectional mass about elastic axis $(k_m^2 = k_{m_1}^2 + k_{m_2}^2)$
k_{m_1}, k_{m_2}	Mass radii of gyration about major neutral axis and about an axis perpendicular to chord through the elastic axis, respectively
M_y, M_z	Resultant moments in y - and z - directions, respectively
m	Mass per unit length
m_t/m_o	Ratio of tip to root mass
n	Number of blade stations
Q	Resultant cross-sectional torque about elastic axis
R	Blade radius
T	Blade tension, $T \cong \int_x^R \Omega^2 mx\, dx$

V_y, V_z	Cross-sectional shears in y- and z-directions
v,w	Lateral displacements of beam, in plane of rotation and normal to plane, respectively
$\bar{v}, \bar{w}$	Vibration amplitude of v and w, respectively
x,y,z	Coordinate system which rotates with blade such that x-axis falls along initial or undeformed position of elastic axis
η	Radial position at which applied loadings are assumed to act
θ	Blade angle prior to any deformation, positive when leading edge is up
λ	Eigenvalue
Φ	Total torsional deflection, $\Phi = \phi_o + \phi$, or eigenvector
ϕ	Elastic torsional deflection, positive when leading edge is up
ϕ_o	Steady-state twist (Appendix B)
$\bar{\phi}$	Vibration amplitude of ϕ
Ω	Rotor angular velocity
ω	Natural frequency of vibration

Primes denote derivatives with respect to x; dots denote derivatives with respect to time

Matrix notation:

[ ]	Square matrix
⌈ ⌋	Diagonal matrix
{ }	Column matrix
$[\ ]^{-1}$	Inverted matrix
[1]	Unit or identity matrix

EQUATIONS OF MOTION

The beam considered in the present analysis is shown in Figure 1. This case represents the coupled bending and torsion of a twisted rotating beam where the elastic axis, mass axis, and tension axis are not necessarily coincident. The free vibration equations of motion for combined bending and torsion are derived in Appendix A in the form

$$(EI_1 \cos^2 \theta + EI_2 \sin^2 \theta)w'' + (EI_2 - EI_1) \cos \theta \sin \theta \, v'' - EB_2\theta'\phi' \sin \theta$$

$$- Te_a \, \phi \cos \theta + \Omega^2 \int_x^R \{m\eta[w(\eta) - w(x)] + me\eta \, \phi \cos \theta\} \, d\eta$$

$$= - \int_x^R (m\ddot{w} + me\ddot{\phi} \cos \theta) \, (\eta - x) d\eta \qquad \text{(1a)}$$

$$(EI_2 - EI_1) \cos \theta \sin \theta \, w'' + (EI_1 \sin^2 \theta + EI_2 \cos^2 \theta)v'' - EB_2 \, \theta'\phi' \cos \theta$$

$$+ Te_a \, \phi \sin \theta + \Omega^2 \int_x^R \{m[xv(\eta) - \eta v(x)] - me\eta\phi \sin \theta\} \, d\eta$$

$$= - \int_x^R (m\ddot{v} - me\ddot{\phi} \sin \theta) \, (\eta - x) d\eta \qquad \text{(1b)}$$

$$[GJ + Tk_a{}^2 + EB_1 \, (\theta')^2]\phi' - EB_2 \, \theta' \, (v'' \cos \theta + w'' \sin \theta) + \int_x^R Te_a \, (v'' \sin \theta$$

$$- w'' \cos \theta) \, d\eta + \Omega^2 \int_x^R [mev \sin \theta + m \, (k_{m_2}{}^2 - k_{m_1}{}^2)\phi \cos 2\theta$$

$$- me\eta \, (v' \sin \theta - w' \cos \theta)] \, d\eta = - \int_x^R [me(\ddot{w} \cos \theta - \ddot{v} \sin \theta)$$

$$+ \ddot{\phi} m \, k_m{}^2] \, d\eta \qquad \text{(1c)}$$

where the variation of the axial tensile force is given by

$$T' + m\,\Omega^2 x = 0 \tag{2}$$

Also, v, w, and ϕ are the edgewise, flapwise, and torsional displacements, respectively. The principal assumptions used in deriving this system of equations are briefly outlined:

(a) The beam is attached to a rigid hub and rotating at constant speed.

(b) The beam elasticity is adequately described by the conventional bending and torsion characteristics described in Reference 1. Furthermore, shear deformation and rotary inertia are assumed to be negligible.

(c) The elastic axis of the undeformed beam is a straight line.

(d) The pitch axis is coincident with the elastic axis of the undeformed beam.

(e) The beam is assumed to have zero precone and prelag.

(f) The cross section is symmetric about the major principal axis.

(g) Cyclic pitch is negligible.

For the present analysis, cantilever-free boundary conditions are assumed. Thus, displacements and slopes are zero at the root:

$$v(0,t) = w(0,t) = \phi(0,t) = v'(0,t) = w'(0,t) = \phi'(0,t) = 0 \tag{3}$$

also, moments and shears are zero at the tip:

$$Q(R,t) = M_y(R,t) = M_z(R,t) = V_y(R,t) = V_z(R,t) = 0 \tag{4}$$

The integrals in Equation (1) may be evaluated by using a matrix operator [L] defined as

$$\left\{ \int_{x_0}^{x_i} f(x)\,dx \right\} = [L]\{f\} \tag{5}$$

Thus, the premultiplication by [L] of a column matrix of the function $f(x)$ yields the integration of $f(x)$ from x_0 to x_i. The $(n + 1)$ matrix [L] is given by Hunter[10] for polynomials of degrees one to seven. For the present analysis, a seventh degree polynomial approximation is used. The matrix [L] avoids solving a set of simultaneous equations since it implicitly contains the polynomial coefficients at each station. By expressing the equations of motion in matrix notation, utilizing the integrating matrix as an operator, and applying the boundary conditions, the equations are formulated into an eigenvalue problem whose solutions may be determined by conventional methods.

The following relationships are valid at each spanwise station:

$$v'(w,t) = v'(0,t) + \int_0^x v''(x,t)\,dx; \quad v(x,t) = v(0,t) + \int_0^x v'(0,t)\,dx \tag{6a}$$

$$w'(x,t) = w'(0,t) + \int_0^x w''(x,t)\,dx; \quad w(x,t) = w(0,t) + \int_0^x w'(w,t)\,dx \tag{6b}$$

$$\phi(x,t) = \phi(0,t) + \int_0^x \phi'(x,t)\,dx \tag{6c}$$

Applying the boundary conditions given by Equation (3) to Equation (6) and using Equation (5) yields

$$\{v'\} = [F]\{v''\}, \quad \{v\} = [F]\{v'\} = [F]^2\{v''\}$$

$$\{w'\} = [F]\{w''\}; \quad \{w\} = [F]\{w'\} = [F]^2\{w''\}$$

$$\{\phi\} = [F]\{\phi'\}$$

where $[F] = \lfloor 1 \rceil [L] \lfloor 1 \rceil$. The first element in the above column vectors is the corresponding quantity at the tip. Assuming simple harmonic motion

$$w(x,t) = \bar{w}(x)e^{i\omega t},\ v(x,t) = \bar{v}(x)e^{i\omega t},\ \phi(x,t) = \bar{\phi}(x)e^{i\omega t}$$

and applying the matrix operator [L] to Equation (1) yields

$$[G]\{\Phi\} = \omega^2[H]\{\Phi\} \tag{7a}$$

where

$$\{\Phi\} = \begin{Bmatrix} \bar{w}'' \\ \bar{v}'' \\ \bar{\phi}' \end{Bmatrix}$$

and

$$[G] = \begin{bmatrix} G_{1_w} & G_{1_v} & G_{1_\phi} \\ G_{2_w} & G_{2_v} & G_{2_\phi} \\ G_{3_w} & G_{3_v} & G_{3_\phi} \end{bmatrix} ; \quad [H] = \begin{bmatrix} H_{1_w} & H_{1_v} & H_{1_\phi} \\ H_{2_w} & H_{2_v} & H_{2_\phi} \\ H_{3_w} & H_{3_v} & H_{3_\phi} \end{bmatrix}$$

Equation (7a) may be expressed in standard eigenvalue form as

$$\lambda\{\Phi\} = [D]\ \{\Phi\} \tag{7b}$$

Where $[D] = [G]^{-1}\ [H]$. Solutions of Equation (7b) define the natural frequencies and associated modal vectors. The first element in the above matrices corresponds to a tip value. In order to satisfy the tip boundary conditions, the 1, n + 1, and 2n + 1 rows and columns of the dynamic matrix [D] are deleted. The partitions of [G] and [H] are (n + 1) matrices defined as follows:

$$[G_{1_w}] = \lceil EI_1 \cos^2 \theta + EI_2 \sin^2 \theta \rfloor + \Omega^2 \, [P_3(mx)[F]^2$$

$$[G_{2_w}] = \lceil (EI_2 - EI_1) \cos \theta \sin \theta \rfloor$$

$$[G_{3_w}] = - \Omega^2 [L] \lceil e_a \cos \theta \rfloor \lceil P_2(mx) \rfloor + \Omega^2 [L] \lceil mex \cos \theta \rfloor [F] - \lceil EB_2 \, \theta' \sin \theta \rfloor$$

$$[G_{1_v}] = \lceil (EI_2 - EI_1) \cos \theta \sin \theta \rfloor$$

$$[G_{2_v}] = \lceil EI_1 \sin^2 \theta + EI_2 \cos^2 \theta \rfloor - \Omega^2 \, [P_1][m] \, [F]^2 + \Omega^2 [P_3(mx)] \, [F]^2$$

$$[G_{3_v}] = \Omega^2 [L] \lceil e_a \sin \theta \rfloor \lceil P_2(mx) \rfloor + \Omega^2 \, [L] \lceil me \sin \theta \rfloor [F]^2 - \Omega^2 [L] \lceil mex \sin \theta \rfloor [F]$$
$$- \lceil EB_2 \, \theta' \cos \theta \rfloor$$

$$[G_{1_\phi}] = - \Omega^2 \lceil P_2(mx) \rfloor \lceil e_a \cos \theta \rfloor [F] + \Omega^2 \, [L] \lceil mex \cos \theta \rfloor [F] - \lceil EB_2 \, \theta' \sin \theta \rfloor$$

$$[G_{2_\phi}] = \Omega^2 \lceil P_2(mx) \rfloor \lceil e_a \sin \theta \rfloor [F] - \Omega^2 \lceil x \rfloor [L] \lceil me \sin \theta \rfloor [F] - \lceil EB_2 \, \theta' \cos \theta \rfloor$$

$$[G_{3_\phi}] = \lceil GJ \rfloor + \lceil EB_1 (\theta')^2 \rfloor + \Omega^2 \lceil k_a^{\,2} \rfloor \lceil P_2(mx) \rfloor + \Omega^2 \, [L] \lceil m(k^2_{m_2} - k^2_{m_1}) \cos 2\theta \rfloor [F]$$

$$[H_{1_w}] = [P_1] \lceil m \rfloor [F]^2$$

$$[H_{2_w}] = [0]$$

$$[H_{3_w}] = [L] \lceil me \cos \theta \rfloor [F]^2$$

$$[H_{1_v}] = [0]$$

$$[H_{2_v}] = [P_1][m][F]^2$$

$$[H_{3_v}] = -[L][me \sin\theta][F]^2$$

$$[H_{1_\phi}] = [P_1]\lceil me \cos\theta \rfloor [F]$$

$$[H_{2_\phi}] = -[P_1]\lceil me \sin\theta \rfloor [F]$$

$$[H_{3_\phi}] = [L]\lceil mk_m^2 \rfloor [F]$$

where

$$[P_1] = [L]\lceil x \rfloor - \lceil x \rfloor [L]$$

$$\lceil P_2(f) \rfloor = \mathrm{diag}\,[L]\{f\}$$

$$[P_3(f)] = [L]\lceil f \rfloor - \lceil P_2(f) \rfloor$$

$$[F] = \lfloor 1 \rceil [L] \lfloor 1 \rceil$$

The modal deflections are determined from the eigenvectors of Equation (7b) as

$$\begin{Bmatrix} \bar{w} \\ \bar{v} \\ \bar{\phi} \end{Bmatrix} = \left[\begin{array}{c|c|c} [F]^2 & & \\ \hline & [F]^2 & \\ \hline & & [F] \end{array}\right] \begin{Bmatrix} \bar{w}'' \\ \bar{v}'' \\ \bar{\phi}' \end{Bmatrix} \qquad (8)$$

Solutions of Equation (7b) are obtained by using the QR transformation method. The dynamic matrix [D] is reduced to upper Hessenberg form by elementary similarity transformations.[15, 16] The similarity transformations, known as QR transformations,[15, 17, 18] of Francis are used iteratively to reduce the matrix to an upper triangular form. The eignevectors corresponding to the real eignevalues are computed by using the inverse interation method of Wielandt (as discussed in Ref. 18).

NUMERICAL EXAMPLES

The results of two free vibration problems are presented to give an indication of the accuracy of the present method of analysis and to show the effects of the variation of certain parameters. The numerical examples considered are a typical propeller blade and a tapered beam having lateral displacements in only one direction. To verify the applicability of the equations of motion to a practical problem, the natural vibration frequencies of the propeller blade were determined numerically and compared with experimental data. The computed results for the tapered beam are compared with exact and approximate solutions.

Tapered Beams

The free vibration characteristics of linearly tapered beams having lateral displacements in one direction are presented to substantiate the accuracy of the solution method. Table 1 gives the comparison of computed and exact-solution bending modes of a nonrotating uniform beam at zero pitch. Table 2 gives a comparison of bending frequencies of linearly tapered beams at zero pitch. The nonrotating uniform beam results correspond to the exact values from Reference 19. The approximate Rayleigh-Southwell method presented in Reference 20 is used to estimate frequencies of the linearly tapered beams. The computed frequencies of the linearly tapered beams are in excellent agreement with the Rayleigh-Southwell method.

Propeller Blade

The propeller blade selected for analysis is the WADC S-5 scale model of Reference 21. This blade was chosen since this reference gives a structural description sufficient for the numerical solution as well as experimental data for the natural vibration frequencies. The blade is in effect cantilevered at 0.1016 meters from the center of rotation and the tip of the blade is at a radius of 0.6096 meters. In the experimental program, tests were conducted for various pitch angles. The pitch settings were defined by the values of θ as measured at $x = 0.75R$ where R is the radius from the center of rotation to the tip of the blade.

In order to compare numerical results with test data, solutions were computed for cases corresponding to the pitch settings and rotational speeds of the experimental investigation. Numerical solutions were obtained by using 11 stations, which correspond to ten 0.0508 meter intervals, to describe the cross-sectional properties of the propeller blade. Physical properties of the WADC S-5 blade, as given in Reference 21, are presented in Table 3. Additional sectional properties needed for this analysis were estimated by assuming an elliptical cross section. These estimated physical properties are presented in Table 4.

The experimentally and analytically determined free vibration frequencies are given in Figures 2 and 3. Figure 2 illustrated the comparison for the first and second bending frequencies. Figure 3 shows the comparison for the first torsion frequency. The computed results of Figure 3 were obtained by using the nonlinear twist analysis of Appendix B. Figure 4 illustrates the effect of steady-state twist on the first torsion natural frequency.

Experimental torsion frequencies are compared with the nonlinear analysis of Appendix B and the linear analysis given by the uncoupled form of Equation (1c). Table 5 gives the percent error associated with each analysis. A comparison of the modal displacements is not possible since the mode shapes were not determined in the experimental investigation.

CONCLUDING REMARKS

A numerical method for determining the free vibration characteristics of a rotating cantilevered blade having nonuniform spanwise properties is presented. By expressing the equations of motion in matrix notation, utilizing the integrating matrix as an operator, and applying the boundary conditions, the equations are formulated into an eigenvalue problem whose solutions may then be determined by conventional methods. Computed results were compared with experimental and analytical data. The comparison indicates that the method of solution yields very accurate results.

APPENDIX A

EQUATIONS OF MOTION

The equations of motion for combined bending and torsion are obtained by application of the theory developed by Houbolt and Brooks.[1] This case represents the coupled bending and torsion of a twisted rotating beam where the elastic axis, mass axis, and tension axis are not necessarily coincident. Figure 5 depicts the position of the elastic axis as a space curve. The applied loadings are shown acting at a radial distance (η) from the axis of rotation. The bending moments produced by these loadings at a radial position (x) are

$$M_y = \int_x^R \left\{ -P_x[w(\eta) - w(x)] + P_z[\eta - x] + q_y \right\} d\eta \tag{A1a}$$

$$M_z = \int_x^R \left\{ -P_x[v(\eta) - v(x)] + P_y[\eta - x] + q_z \right\} d\eta \tag{A1b}$$

$$M_t = \int_x^R \left\{ P_x[(w(\eta) - w(x)) \frac{\partial v}{\partial x} - (v(\eta) - v(x)) \frac{\partial w}{\partial x}] - P_y[(w(\eta) - w(x)) \right.$$

$$- (\eta - x) \frac{\partial w}{\partial x}] + P_z[(v(\eta) - v(x)) - (\eta - x) \frac{\partial v}{\partial x}] \tag{A1c}$$

$$\left. + [q_x + q_y \frac{\partial v}{\partial x} + q_z \frac{\partial w}{\partial x} \right\} d\eta$$

For the present analysis, blade elasticity may be adequately described by the conventional bending and torsion characteristics developed in Reference 1. Thus, the elastic restoring moments at an arbitrary radial position (x) are

$$M_y = (EI_1 \cos^2\theta + EI_2 \sin^2\theta)w'' + (EI_2 - EI_1)\sin\theta\cos\theta\, v'' \tag{A2a}$$

$$- (Te_a + EB_2\theta'\phi')\sin\theta - Te_a\,\phi\cos\theta$$

$$M_z = (EI_1 \sin^2\theta + EI_2 \cos^2\theta)v'' + (EI_2 - EI_1)\sin\theta\cos\theta\, w''$$

$$- (Te_a + EB_2\,\theta'\phi')\cos\theta + Te_a\,\phi\sin\theta \tag{A2b}$$

$$M_t = [GJ + Tk_a^2 + EB_1(\theta')^2]\,\phi' + Tk_a^2\,\theta'$$

$$- EB_2\,\theta'\,(v''\cos\theta + w''\sin\theta) \tag{A2c}$$

Equation (A1c) may be written as

$$\frac{\partial M_t}{\partial x} = -q_x - q_y\,v' - q_z\,w' - M_y\,v'' + M_z\,w'' \tag{A3}$$

substituting Equations (A2a) and (A2b) and neglecting products of elastic deflections yields

$$\frac{\partial M_t}{\partial x} = -q_x - q_y v' - q_z w' + Te_a\,v''\sin\theta - Te_a w''\cos\theta \tag{A4}$$

Combining Equations (A1), (A2), (A4) and substituting the applied loadings given by Equation (21) of Reference 1 yields

$$(EI_1 \cos^2 \theta + EI_2 \sin^2 \theta)w'' + (EI_2 - EI_1) \cos \theta \sin \theta\, v''$$

$$- EB_2\, \theta'\phi' \sin \theta - Te_a\, \phi \cos \theta + \Omega^2 \int_x^R \{m\eta[w(\eta) - w(x)]$$

$$+ me\eta\, \phi \cos \theta\}\, d\eta \;=\; - \int_x^R (m\ddot{w} + me\ddot{\phi} \cos \theta)\, (\eta - x)d\eta$$

$$(EI_2 - EI_1)\cos \theta \sin \theta\, w'' + (EI_1 \sin^2 \theta + EI_2 \cos \theta)v'' - EB_2\, \theta'\phi' \cos \theta$$

$$+ Te_a\, \phi \sin \theta + \Omega^2 \int_x^R \{m[xv(\eta) - \eta v(x)] - me\eta\phi \sin \theta\}\, d\eta \qquad \text{(A5b)}$$

$$= - \int_x^R (m\ddot{v} - me\ddot{\phi} \sin \theta)\, (\eta - x)d\eta$$

$$[GJ + Tk_a{}^2 + EB_1\, (\theta')^2]\phi' - EB_2\, \theta'\, (v'' \cos \theta + w'' \sin \theta) + \int_x^R Te_a\, (v'' \sin \theta$$

$$- w'' \cos \theta)\, d\eta + \Omega^2 \int_x^R [mev \sin \theta + m\, (k_{m_2}{}^2 - k_{m_1}{}^2)\phi \cos 2\theta$$

$$- me\eta\, (v' \sin \theta - w' \cos \theta)]\, d\eta = - \int_x^R [me(\ddot{w} \cos \theta - \ddot{v} \sin \theta)$$

$$+ \ddot{\phi} m\, k_m{}^2]\, d\eta$$

APPENDIX B

STEADY-STATE TWIST OF ROTATING BLADES

Equation (1) is valid for small displacements from the undeformed configuration of the nonrotating blade. The angle θ at any radial station x, defines the orientation of the major principal axis relative to the plane of rotation. Thus, the local orientation of the nonrotating blade includes pitch and pretwist. However, the local orientation of a blade segment may be modified due to the presence of rotation. This effect is defined as "steady-state" twist and is a function of blade characteristics and rotational speed.

An approximate estimate of the steady-state twist may be obtained by assuming that blade torsional response is uncoupled. The uncoupled linear torsional restoring moment is given by

$$M_t = [GJ + Tk_a^2 + EB_1(\theta')^2]\phi' + Tk_a^2\,\theta' \qquad \text{(B1)}$$

Equation (B1) is valid for $v = w = 0$, and ϕ a small angle. However, the presence of steady-state twist may invalidate the assumption of small angular displacement from the undeformed position. The equivalent form of Equation (B1) for $v = w = 0$, and large angular displacement is (see Appendix A, Ref. 1)

$$M_t = \{GJ + EB_1[(\theta')^2 + \frac{3}{2}\;\theta'\Phi' + \frac{1}{2}\,(\Phi')^2]\}\Phi' + Tk_a^2\,(\theta' + \Phi') \qquad \text{(B2)}$$

where Φ is the sum of the steady-state twist, ϕ_0, and the torsional elastic deformation ϕ.

$$\Phi(x,t) = \phi_0(x) + \phi(x,t) \tag{B3}$$

Using Equation (B2) the uncoupled torsional equation is

$$\{GJ + EB_1[(\theta')^2 + \frac{3}{2}\theta'\Phi' + \frac{1}{2}(\Phi')^2]\}\Phi' + Tk_a^2(\theta' + \Phi')$$

$$+ \frac{\Omega^2}{2}\int_x^R m(k_{m_2}^2 - k_{m_1}^2)\sin 2(\theta + \Phi)\, d\eta + \int_x^R mk_m^2\ddot{\Phi}\, d\eta = 0 \tag{B4}$$

Substituting Equation (B3) into Equation (B4) and setting all perturbation quantities equal to zero yields the equilibrium equation

$$\{GJ + EB_1[(\theta')^2 + \frac{3}{2}\theta'\phi_o' + \frac{1}{2}(\phi_o')^2]\}\phi_o' + Tk_a^2(\theta' + \phi_o')$$

$$+ \frac{\Omega^2}{2}\int_x^R m(k_{m_2}^2 - k_{m_1}^2)\sin 2(\theta + \phi_o)\, d\eta = 0 \tag{B5}$$

Substituting Equation (B3) into Equation (B4), subtracting the equilibrium equation and discarding higher order products of perturbation quantities, yields the perturbation equation.

$$\{GJ + Tk_a^2 + EB_1[(\theta')^2 + 3\theta'\phi_o' + \frac{3}{2}(\phi_o')^2]\}\phi'$$

$$+ \Omega^2\int_x^R m(k_{m_2}^2 - k_{m_1}^2)\phi\cos 2(\theta + \phi_o)\, d\eta + \int_x^R m\, k_m^2\ddot{\phi}\, d\eta = 0 \tag{B6}$$

The steady-state twist ϕ_o is determined by iteration from Equation (B5). This value is used to determine the coefficients of Equation (B6) which is solved for the uncoupled torsional frequencies.

REFERENCES

1. Houbolt, John C., and Brooks, George W.: Differential Equations of Motion for Combined Flapwise Bending, Chordwise Bending, and Torsion of Twisted Nonuniform Rotor Blades. NACA Rep. 1346, 1958.

2. Isakson, G., and Eisley, J. G.: Natural Frequencies in Bending of Twisted Rotating Blades. NASA TN D-371, March 1960.

3. Isakson, G., and Eisley, J. G.: Natural Frequencies in Coupled Bending Torsion of Twisted Rotating and Nonrotating Blades. NASA CR-65, 1964.

4. Berman, Alex: A New Approach to Rotor Blade Dynamic Analysis. J. Amer. Helicopter Soc., Vol. 10, No. 3, July 1965, pp. 15-29.

5. Lipeles, Jay L.: Vibrations of a Rotating Beam. J. Amer. Helicopter Soc., Vol. II, No. 4, October 1966, pp. 17-24.

6. Montoya, J.: Coupled Bending and Torsional Vibration in a Twisted Rotating Blade. Brown Boveri Review, Vol. 53, No. 3, March 1966, pp. 216-230.

7. Vakhitov, M. B.: Integrating Matrices as a Means of Numerical Solution of Differential Equations in Structural Mechanics. Izvestiya VUZ. Aviatsionnaya Tekhnika, No. 3, 1966, pp. 50-61.

8. Arcidiacono, P. J.: Steady Flight Differential Equations of Motion for a Flexible Helicopter Blade With Chordwise Mass Unbalance. USAAVLABS TR 68-18A, 1969.

9. Piziali, R. A.: An Investigation of the Structural Dynamics of Helicopter Rotors. USAAVLABS TR 70-24, April 1970.

10. Hunter, William F.: Integrating-Matrix Method for Determining the Natural Vibration Characteristics of Propeller Blades. NASA TN D-6064, December 1970.

11. Rawtani, S., and Dikainish, M. A.: Natural Frequencies of Rotating, Low Aspect Ratio, Turbomachinery Blades. AIAA Paper No. 71-374, AIAA/ASME 12th Structures, Structural Dynamics and Materials Conference, April 1971.

12. Liss, A. Y.: Equations of Propeller Blade Deformation and the Orthogonality Properties of the Pattern of Its Oscillations. Izvestiya VUZ. Aviatsionnaya Tekhnika, Vol. 15, No. 4, 1972, pp. 56-66.

13. Sadler, Gene S.: Program Documentation for Blade Frequency Program for Nonuniform Helicopter Rotors, With Automated Frequency Search. NASA CR-112071, 1972.

14. Oette, H.: Calculation of the Flapwise Bending, Edgewise Bending, and Torsional Vibrations of Rotor Blades With Coupled Natural Modes and Frequencies. NASA TT F-16,004, November 1974.

15. Wilkinson, J. H.: Stability of the Reduction of a Matrix to Almost Triangular Forms by Elementary Similarity Transformations. J. Assoc. Comput. Mach., Vol. 6, 1959, pp. 336-359.

16. Fox, L.: An Introduction to Numerical Linear Algebra. Oxford Univ. Press, 1965.

17. Francis, J. G. F.: The QR Transformation--A Unitary Analogue to the LR Transformation. Comput. J., Vol. 4. Pt. 1 - Oct. 1961, pp. 265-271. Pt. 2 - Jan. 1962, pp. 332-345.

18. Wilkinson, J. H.: The Algebraic Eigenvalue Problem. Clarendon Press (Oxford), 1965.

19. Chang, T. -C, and Craig, R. R., Jr.: On Normal Modes of Uniform Beams. EMRL 1068, The University of Texas at Austin, January 1969.

20. Yntema, Robert T.: Simplified Procedures and Charts for the Rapid Estimation of Bending Frequencies of Rotating Beams. NACA TN 3459, June 1955.

21. Carpenter, J. E., and Sullivan, E. M.: Structural and Vibrational Characteristics of WADC S-5 Model Propeller Blades. WADC TR 56-298, June 1957.

TABLE 1. COMPARISON OF COMPUTER AND EXACT-SOLUTION VALUES OF BENDING DISPLACEMENTS FOR A UNIFORM BLADE, $\Omega = 0$, $\theta = 0$.

	COMPUTED			EXACT SOLUTION REFERENCE (19)		
x/R	$\bar{w}_1$	$\bar{w}_2$	$\bar{w}_3$	$\bar{w}_1$	$\bar{w}_2$	$\bar{w}_3$
0.0	.0	.0	.0	.0	.0	.0
0.1	.0168	.0926	.2276	.0168	-.0926	.2281
0.2	.0639	-.3011	.6040	.0639	-.3011	.6045
0.3	.1365	-.5261	.7558	.1368	-.5261	.7562
0.4	.2299	-.6835	.5261	.2299	-.6835	.5259
0.5	.3395	-.7137	.0204	.3395	-.7137	.0197
0.6	.4611	-.5895	-.4729	.4611	-.5895	-.4738
0.7	.5909	-.3171	-.6569	.5909	-.3171	-.6574
0.8	.7255	.0700	-.3949	.7255	.0700	-.3949
0.9	.8624	.5238	.2280	.8624	.5238	.2285
1.0	1.0000	1.0000	1.0000	1.0000	1.0000	1.0000

TABLE 2. BENDING FREQUENCIES OF LINEARLY TAPERED BLADES, $\theta = 0$.

m_t/m_o	EI_t/EI_o	Ω rpm	COMPUTED HZ.			RAYLEIGH-SOUTHWELL APPROXIMATION REF. (20), HZ.		
			ω_1	ω_2	ω_3	ω_1	ω_2	ω_3
1.0	1.0	0 300	1.426 5.47	8.935 15.[illegible]	25.00 32.6	1.426 5.53	8.935 15.4	25.00 32.5
1.0	0.5	0 300	1.35 5.47	7.9 14.9	21.6 29.9	1.35 5.66	7.9 14.8	21.8 29.7
1.0	0.0	0 300	1.25 5.46	6.3 14.2	16.1 25.8	1.22 5.74	6.4 14.1	16.1 25.4
0.5	1.0	0 300	1.85 5.64	10.7 16.0	29.4 35.3	1.86 5.75	10.7 15.9	29.1 34.6
0.5	0.5	0 300	1.75 5.62	9.5 15.3	25.6 32.0	1.76 5.77	9.5 15.1	25.6 31.7
0.5	0.0	0 300	1.62 5.61	7.8 14.2	19.4 26.9	1.62 5.82	7.6 14.0	19.4 26.8
0.0	1.0	0 300	3.21 6.28	16.2 19.4	42.6 45.9	3.20 6.29	16.2 19.2	42.0 44.9
0.0	0.5	0 300	3.07 6.23	14.7 18.1	37.8 41.4	3.04 6.25	14.7 17.9	37.6 40.7
0.0	0.0	0 300	2.89 6.18	12.5 16.4	30.5 34.6	2.88 6.23	12.4 16.1	30.4 34.1

TABLE 3. PHYSICAL PROPERTIES OF PROPELLER BLADE

(Cantilevered at 0.1524 m; station length 0.0508 m)

X/R	m, $N\text{-}sec^2/m^2$	EI_1, $N\text{-}m^2$	EI_2, $N\text{-}m^2$	θ, deg	THICKNESS, m	CHORD, m
1.0	3.411	0.689×10^2	1.607×10^5	-10.0	0.3653×10^{-4}	.1691
.9	3.411	.718	1.475	- 7.4	.3587	.1662
.8	3.563	.746	1.355	- 4.1	.3632	.1618
.7	3.638	.775	1.274	0.0	.3759	.1574
.6	3.789	.918	1.257	4.8	.4064	.1537
.5	3.942	1.205	1.257	9.9	.4343	.1489
.4	4.245	1.636	1.274	14.7	.5004	.1439
.3	4.348	2.353	1.314	20.0	.5740	.1405
.2	4.927	3.301	1.375	25.4	.6579	.1354
.1	7.125	9.959	1.834	30.9	.8433	.1308

TABLE 4. ESTIMATED PHYSICAL PROPERTIES OF PROPELLER BLADE ASSUMING ELLIPTICAL CROSS SECTION

X/R	GJ, $N\text{-}m^2$	$k_m = k_a$, m	k_{m_1}, m	k_{m_2}, m	B_1, m^6	B_2, m^5
1.0	1.225×10^2	0.0422	9.119×10^{-4}	0.0422	1.547×10^{-9}	0.0
.9	1.139	.0414	8.966	.0414	1.394	0.0
.8	1.154	.0404	9.068	.0404	1.235	0.0
.7	1.239	.0394	9.398	.0394	1.142	0.0
.6	1.538	.0384	10.160	.0384	1.066	0.0
.5	1.819	.0373	10.846	.0373	.975	0.0
.4	2.678	.0361	12.522	.0356	.945	0.0
.3	3.958	.0351	14.351	.0348	.964	0.0
.2	5.668	.0338	15.459	.0338	.916	0.0
.1	11.626	.0328	21.108	.0325	.988	0.0

TABLE 5. COMPARISON OF EXPERIMENTAL AND ANALYTICAL TORSION FREQUENCY

θ @ .75R DEG	Ω rpm	ω, Hz EXPERIMENTAL	ω, Hz COMPUTED LINEAR	ω, Hz COMPUTED NONLINEAR	PERCENT ERROR LINEAR	PERCENT ERROR NONLINEAR
-20	1586	201.4	209.7	203.8	4.1	1.2
	2554	198.1	214.8	199.8	8.4	.8
	3587	192.7	222.9	194.4	15.7	.9
	4449	188.2	231.7	190.0	23.1	1.0
	5134	186.8	239.9	187.6	28.4	.4
0	1600	203.9	210.2	206.1	3.1	1.1
	2610	203.9	216.1	206.0	6.0	1.0
	3585	204.5	224.3	206.5	10.0	1.0
	5886	214.1	251.5	205.7	17.5	.7
20	1572	205.8	209.7	207.7	1.9	.9
	2542	207.5	214.8	209.8	3.5	1.1
	4476	216.3	231.0	218.1	6.8	.8
	6016	226.1	248.4	229.8	9.9	1.6
40	1482	205.3	208.6	207.6	1.6	1.1
	2536	207.6	212.5	209.9	2.4	1.1
	5975	223.4	236.7	226.7	5.9	1.5
60	1491	204.6	207.6	206.4	1.5	.9
	2682	204.1	210.0	206.2	2.9	1.0
	4523	204.8	215.9	205.8	5.4	.5
	5945	202.4	221.8	205.6	9.6	1.6

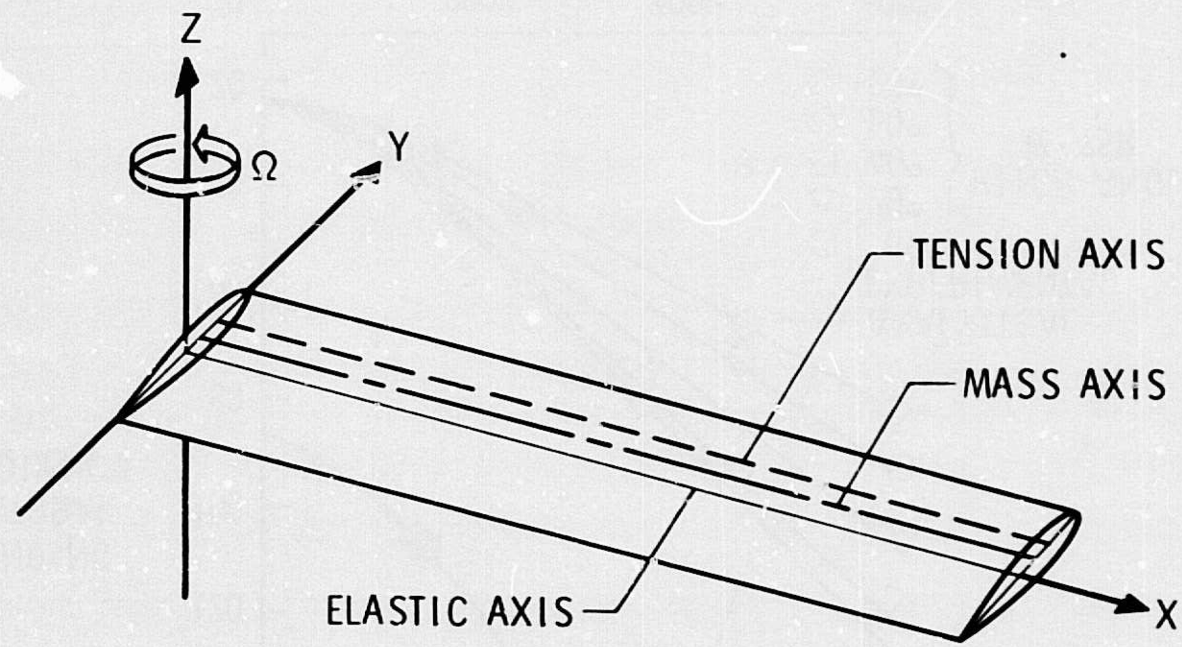

Figure 1. - Undeformed coordinate system.

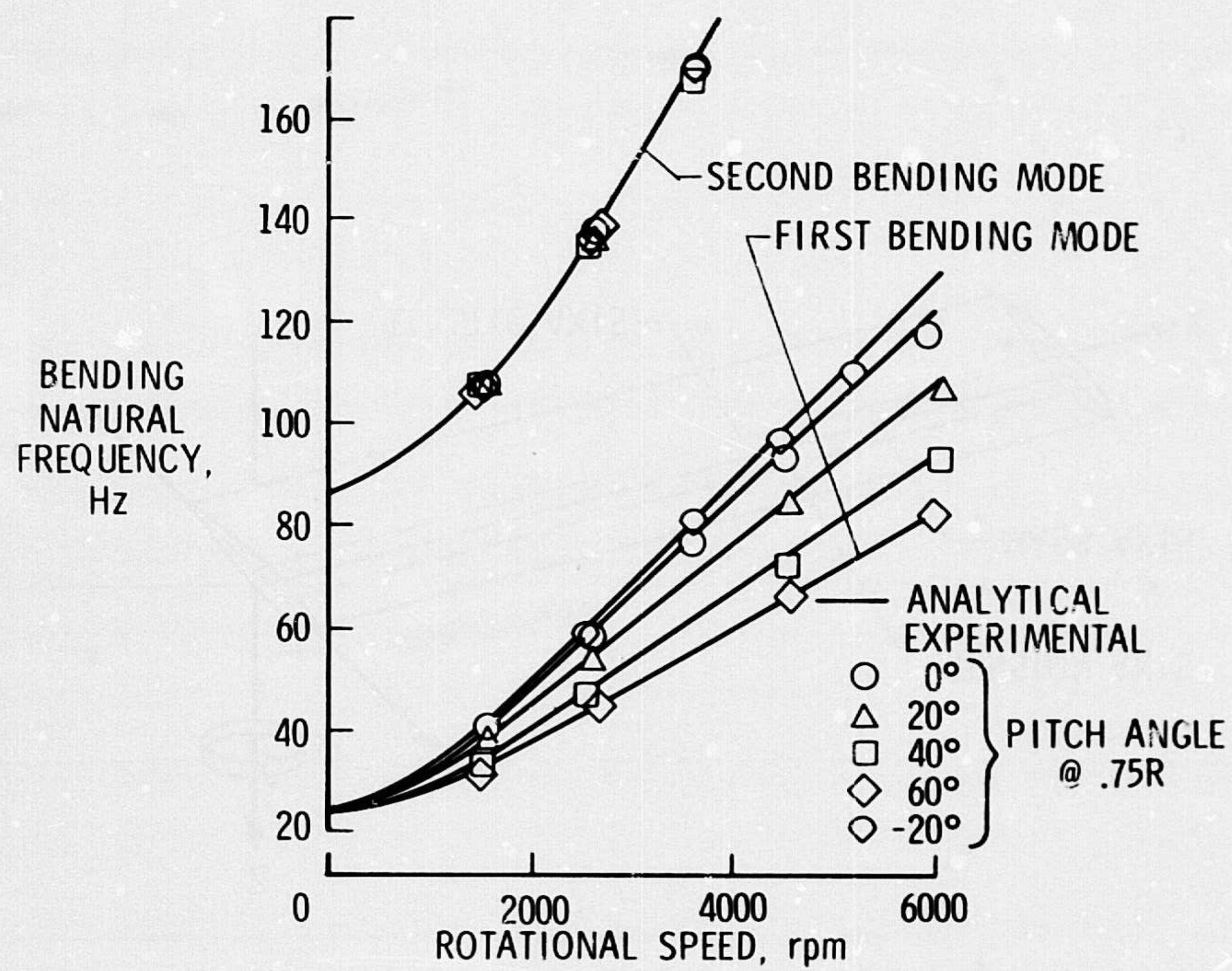

Figure 2. - Variation of bending frequencies with rotational speed.

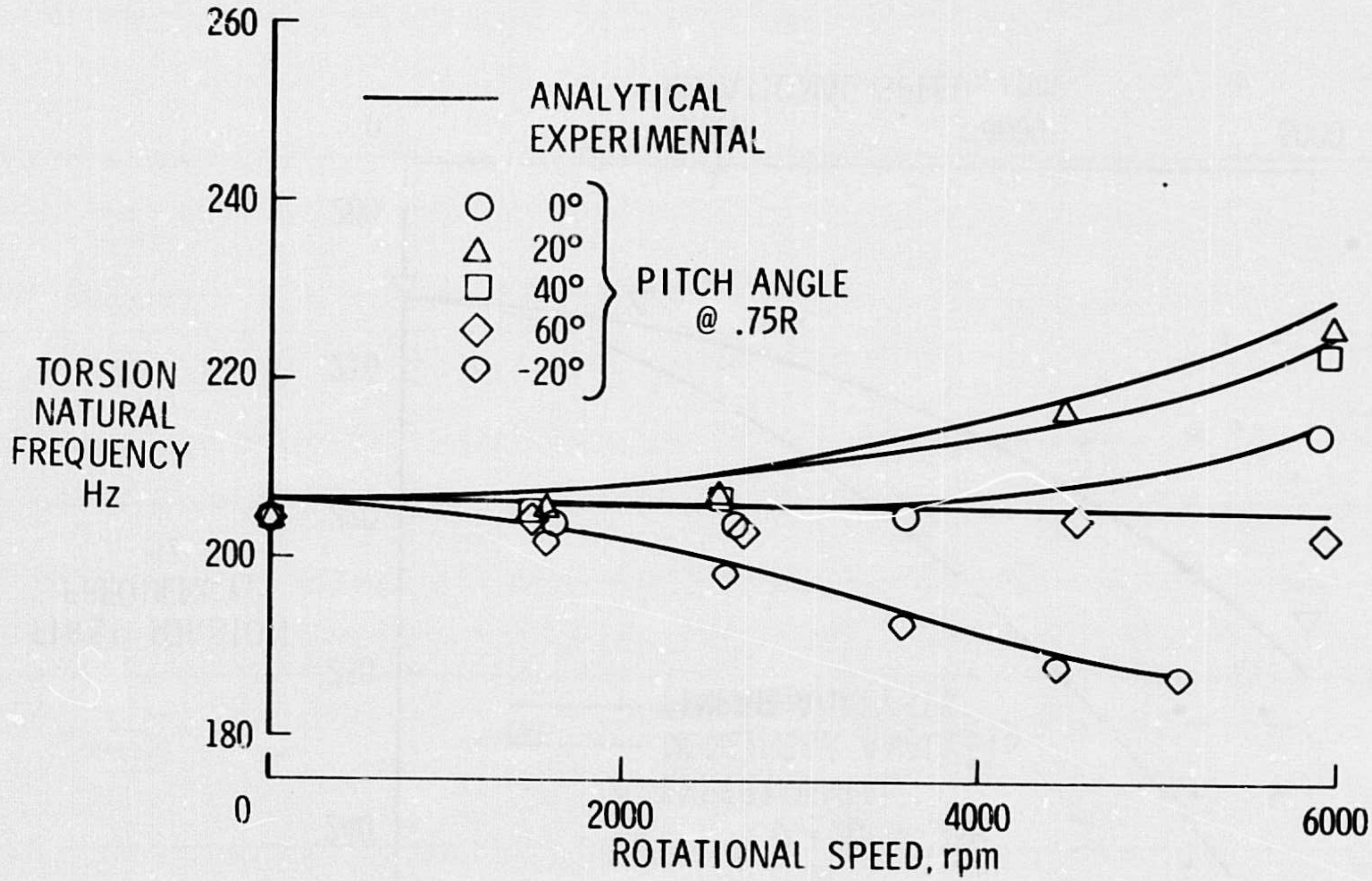

Figure 3. - Variation of torsion frequency with rotational speed.

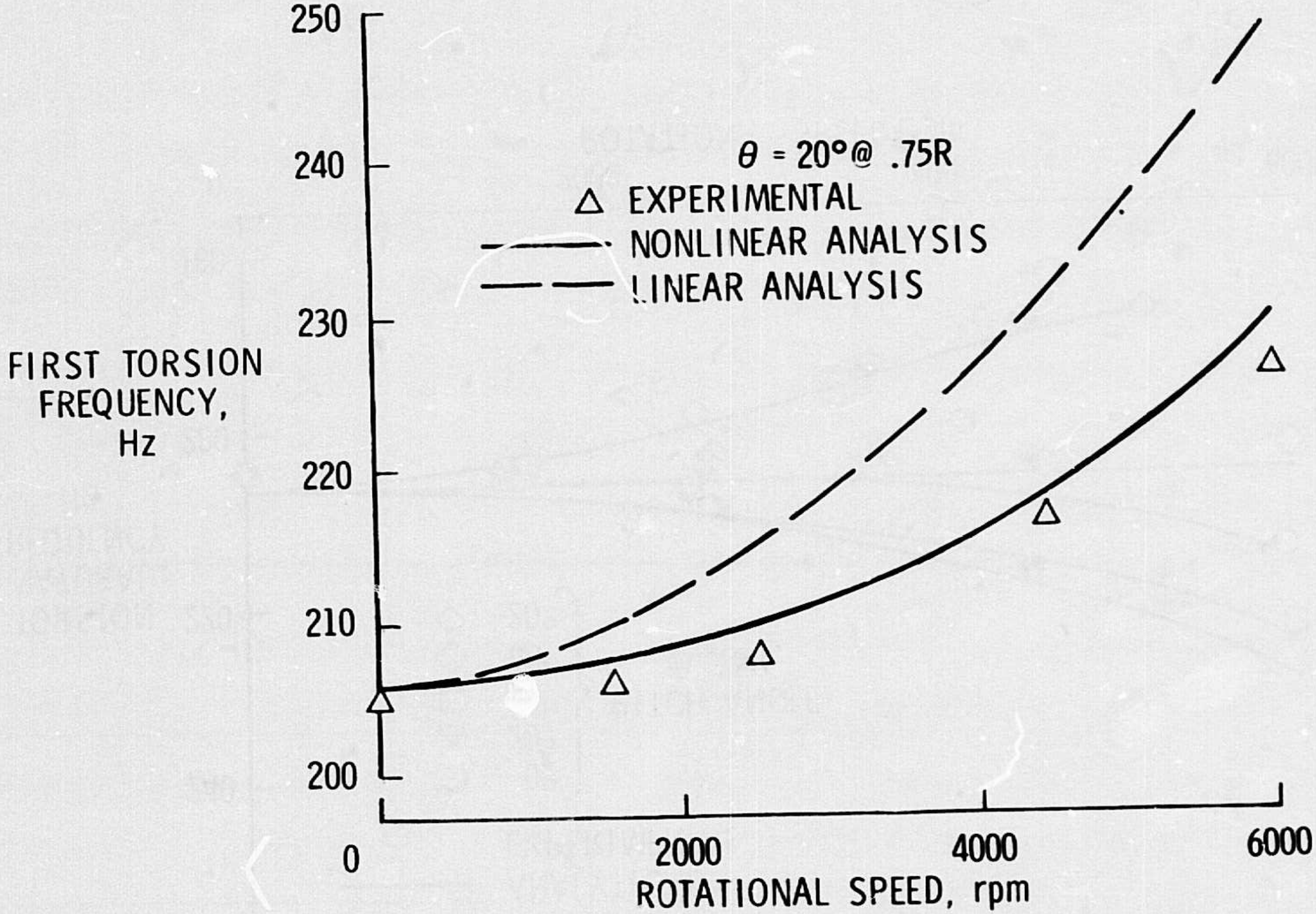

(a) θ = 20° at 0.75R.

Figure 4. - Torsional frequency versus rotational speed.

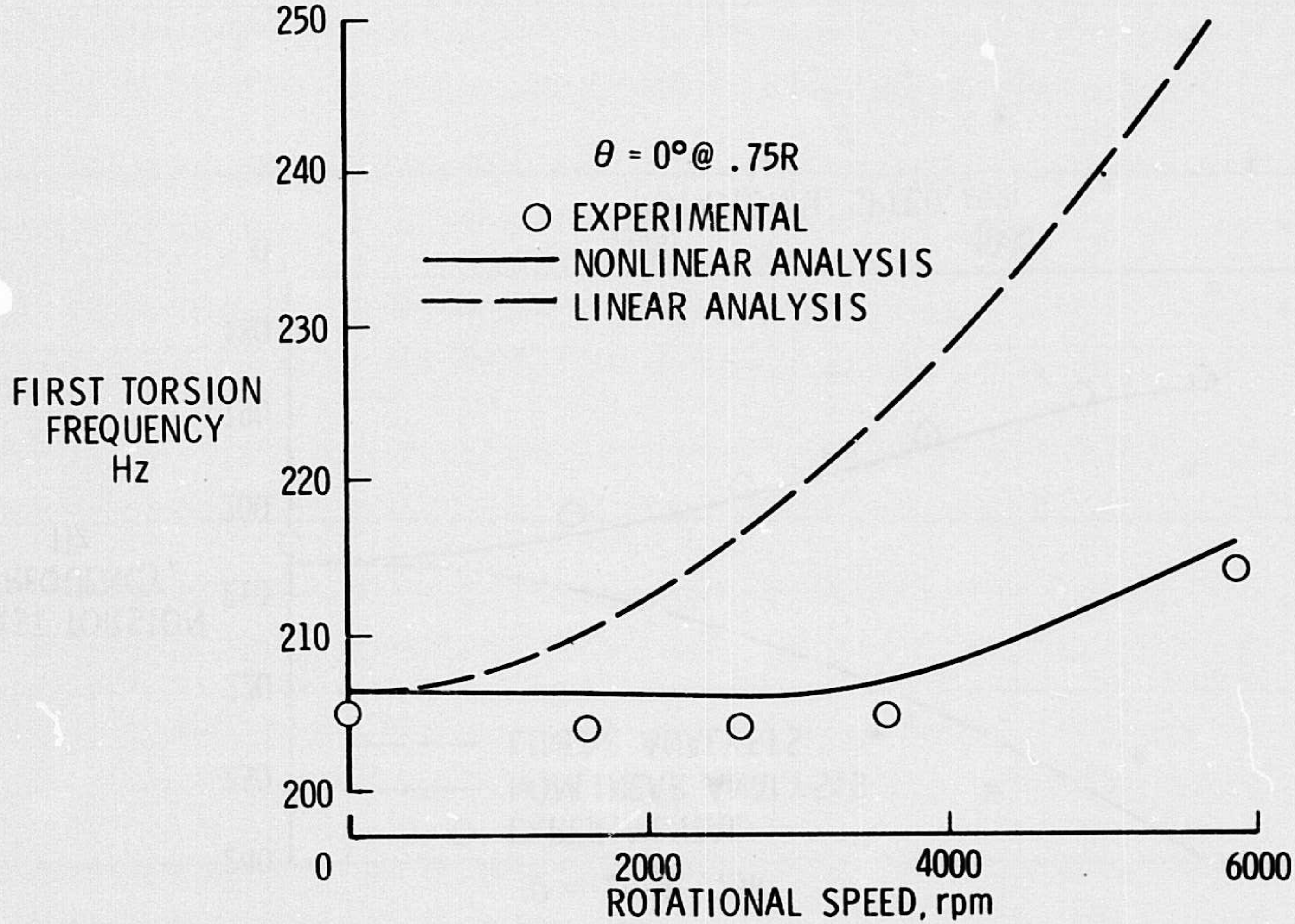

(b) $\theta = 0°$ at 0.75R.

Figure 4. - Continued.

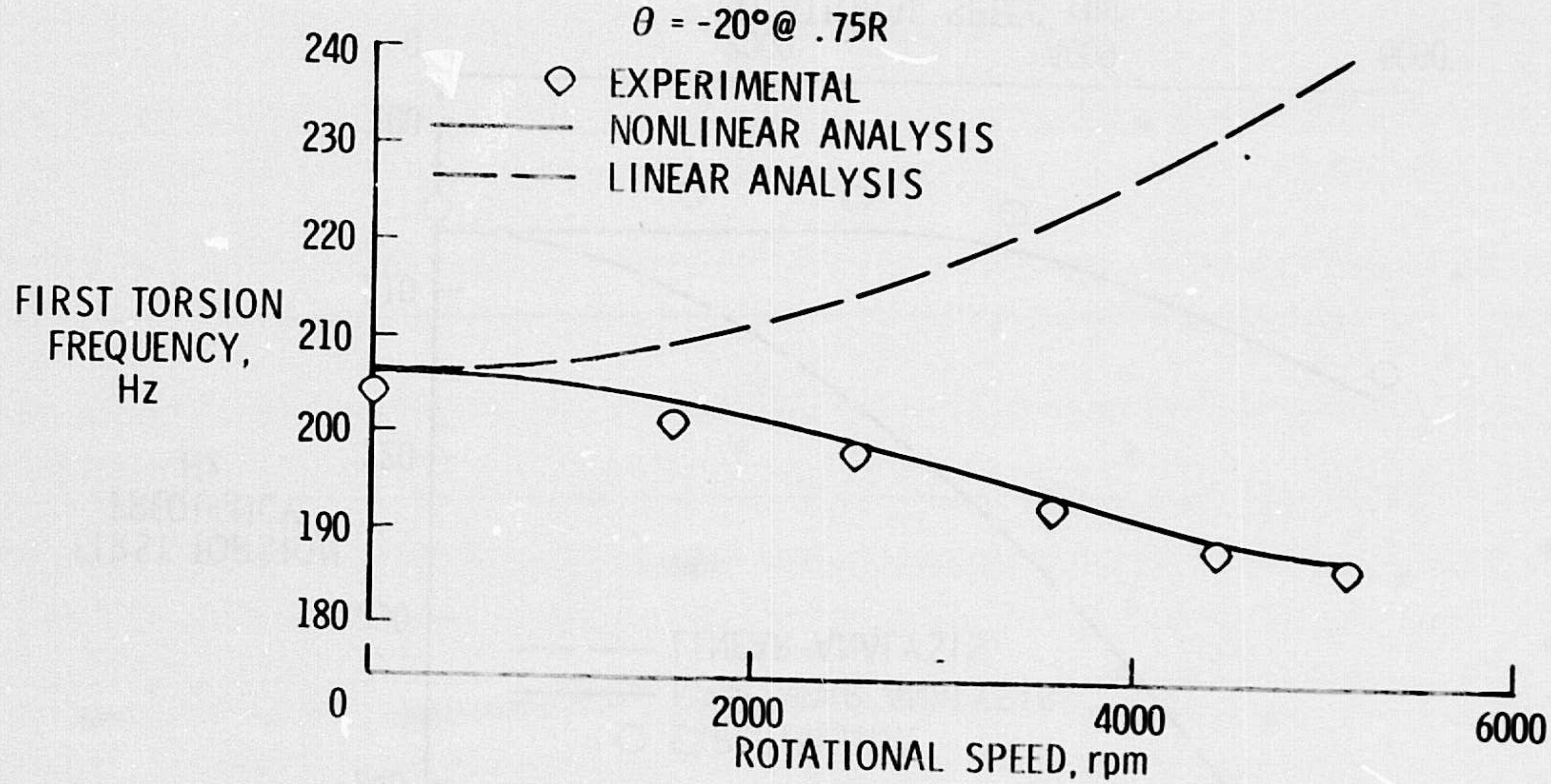

(c) $\theta = -20°$ at 0.75R.

Figure 4. - Concluded.

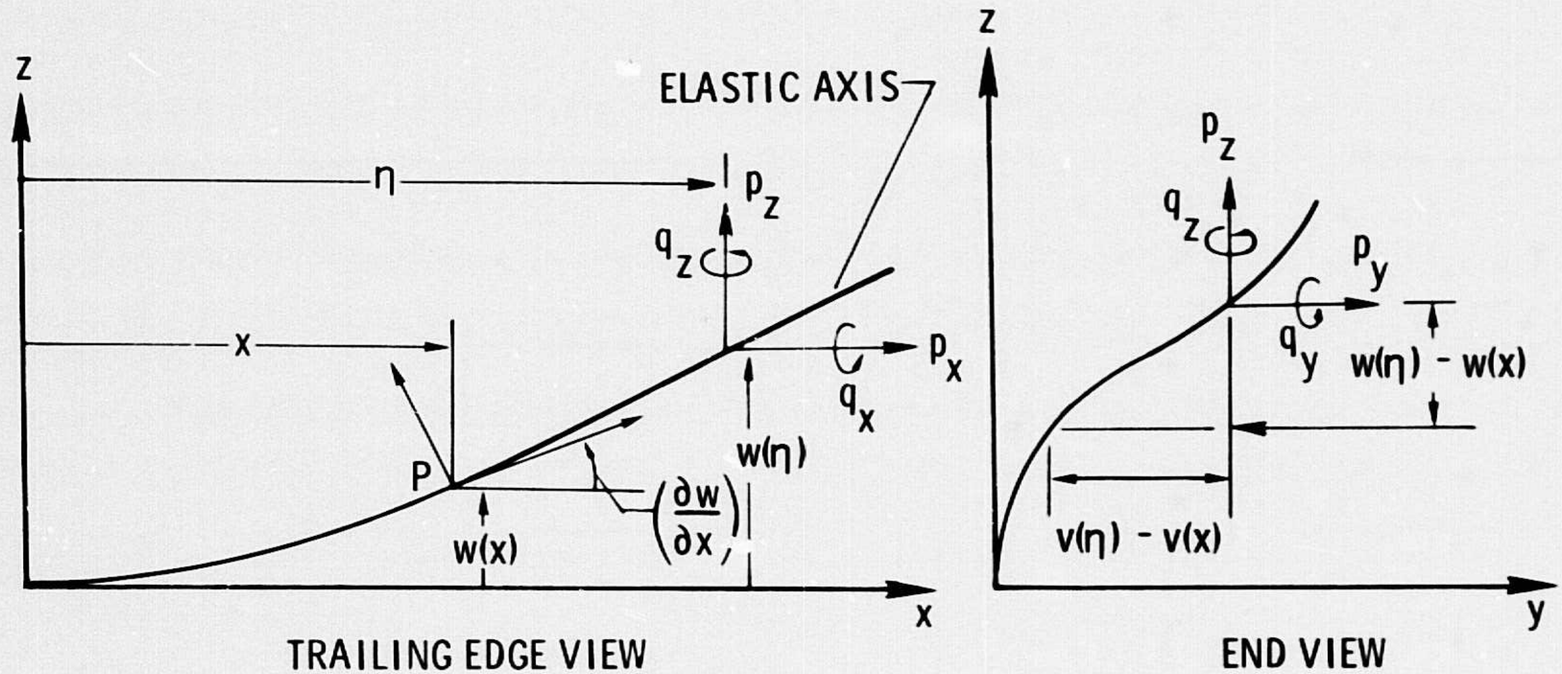

Figure 5. - Equilibrium of forces and moments.